Solving High Order Ordinary Differential Equations with Radial Basis Function Networks

N. Mai-Duy*

School of Aerospace, Mechanical and Mechatronic Engineering,

The University of Sydney, NSW 2006, Australia

Submitted to *Int. J. Numer. Meth. Engng*, January 2004; revised July 2004

*Telephone +61 2 9351 7151, Fax +61 2 9351 7060, E-mail nam.maiduy@aeromech.usyd.edu.au

SUMMARY

This paper is concerned with the application of radial basis function networks (RBFNs) for numerical solution of high order ordinary differential equations (ODEs). Two unsymmetric RBF collocation schemes, namely the usual direct approach based on a differentiation process and the proposed indirect approach based on an integration process, are developed to solve high order ODEs directly and the latter is found to be considerably superior to the former. Good accuracy and high rate of convergence are obtained with the proposed indirect method.

KEYWORDS: RBFNs; approximation; high order; derivatives; ordinary differential equations.

1 INTRODUCTION

The mathematical modelling of many problems in science and engineering leads to ordinary differential equations (ODEs). Depending upon the form of the boundary conditions to be satisfied by solution, problems involving ODEs can be divided into two main categories, namely initial value problems (boundary conditions prescribed at one end of the domain of analysis) and boundary value problems (boundary conditions prescribed at both ends of the domain of analysis). Analytic solutions for these problems are not generally available and hence numerical methods must be resorted to. The traditional numerical methods (Dahlquist et al [1] and Press et al [2]) consist of two stages. At the first stage, new variables are introduced to transform the governing high order ODEs into coupled sets of first order differential equations. At the second stage, the domain of interest is divided into a number of intervals over which the equivalent first order systems obtained from the first stage are integrated for a numerical solution.

For initial value problems, considering an ith interval with two extreme points $x^{(i)}$ and $x^{(i+1)}$. The solution is assumed to be known at $x^{(i)}$ and the solution at $x^{(i+1)}$ is then found by integrating the governing ODEs over the interval i. Note that the solution at $x^{(i)}$ is taken using an initial solution if $i = 1$ or the solution at the second end-point of the immediately preceding interval $(i-1)$ if $i > 1$. Errors can thus tend to accumulate and cause the solution to recede from the exact solution. Depending on the way of integrating ODEs over finite intervals, there are different numerical methods available in literature, for example, the Euler's method, the Runge-Kutta method and the Bulirsch-Stoer method (Dahlquist et al [1] and Press et al [2]).

For boundary value problems, which are generally more difficult than initial value problems, two methods, namely the shooting method and the relaxation method, are often preferred. In the shooting method, an appropriate set of freely specifiable

values is introduced at the starting point to convert the boundary value problem into the initial value problem, from which the initial value methods can be applied. In addition, the Newton-Raphson technique is employed to compute those unspecified initial values by satisfying the boundary conditions at the other boundary point. In the relaxation method, first order ODEs are replaced by finite difference equations on a mesh of points that covers the range of integration, which yield the system of algebraic equations. Further details can be found in many textbooks (e.g. Dahlquist et al [1] and Press et al [2]).

The transformation of the governing high order ODEs into coupled sets of first order ODEs can result in relatively large requirements for memory and computation. On the other hand, it is possible to develop other numerical methods capable of solving high order ODEs directly in an effective and efficient manner. In this regard, many attempts based on high order approximation schemes were made (e.g. Viecelli [3]; Sallam and El-Hawary [4]; Esmail et al [5]; Gutierrez and Laura [6]; Wu and Liu [7,8,9]). For example, the Cauchy problems governed by second order and fourth order equations were solved successfully using deficient spline function approximations by Sallam and El-Hawary [4] and Esmail et al [5] respectively. Recently, the differential quadrature (DQ) method (Bellman and Casti [10]) was developed to solve fourth, sixth and eighth order ODEs without using the δ-point technique for the treatment of multiple boundary conditions in the papers of Wu and Liu [8,7,9] respectively. Note that the construction of a finite difference or finite element approximation (i.e. low order methods) to high order ODEs is not a trivial task (Viecelli [3]; Wood and Morton [11]). This paper presents alternative high order methods based on radial basis function networks (RBFNs) for solving ODEs directly. In the proposed method, the well-known difficulties in dealing with multiple boundary conditions are naturally overcome via a means of the integration process associated with the process of deriving new basis functions.

The concept of solving DEs by using RBFNs was first introduced by Kansa [12]. Since then, it has received a great deal of attention from researchers. As a result, many further interesting developments and applications have been reported (e.g. Sharan et al [13]; Zerroukat et al [14]; Mai-Duy and Tran-Cong [15,16]; Fedoseyev et al [17]). Essentially, in a typical RBF collocation method, each variable and its derivatives are all expressed as weighted linear combinations of basis functions, where the sets of network weights are identical. These closed form representations are substituted into the governing equations as well as boundary conditions, and the point collocation technique is then employed to discretize the system. If all basis functions in networks are available in analytic forms, the RBF collocation methods can be regarded as truly meshless methods. There are two basic approaches for obtaining new basis functions from RBFs, namely the direct approach (DRBF) based on a differential process (Kansa [12]) and the indirect approach (IRBF) based on an integration process (Mai-Duy and Tran-Cong [15,18]). Both approaches were tested on the solution of second order DEs and the indirect approach was found to be superior to the direct approach (Mai-Duy and Tran-Cong [15]). In this paper, they are further developed for solving high order ODEs without prior conversion into the equivalent systems of first order ODEs. In contrast to the traditional methods, the domain of analysis in the present procedures using multiquadrics is discretized into a number of distinct points (instead of a number of intervals) since there are no intervals required for both processes: integration of ODEs and interpolation of the field variable (see Jin, Li and Aluru [19], Atluri and Shen [20], Li and Liu [21] and Liu [22] for an overview on meshless methods). It should be emphasized that the integration process here is employed only for the purpose of deriving new basis functions from RBFs. The case of using the integration formulations (weak-form/inverse statement) with the direct RBF interpolation schemes can be found in, for example, Liu and Gu [23], Wang and Liu [24,25], Wang et al [26], Gu and Liu [27] and Wu and Liu [28]. Numerical examples show that the proposed method

gives accurate results using relatively low numbers of data points.

The paper is organized as follows. In section 2, the direct and indirect RBFN approaches for the approximation of high order derivatives are presented. Analytic and numerical techniques for obtaining new basis functions from RBFs are discussed in Section 3. Section 4 is to demonstrate the workings of the RBF collocation methods in the solution of high order ODEs. The present methods are then verified through a number of numerical examples in section 5, which are first carried out for the approximation of derivative functions and then for boundary value, eigenvalue and initial value problems governed by fourth, sixth and eighth order ODEs. Section 6 gives some concluding remarks. In the appendix, the analytic form of new basis functions used in the direct and indirect approaches is given.

2 RADIAL BASIS FUNCTION NETWORKS

An 1D function $y(x)$ to be interpolated or approximated can be represented by an RBF network as follows (Haykin [29])

$$y(x) \approx f(x) = \sum_{i=1}^{m} w^{(i)} g^{(i)}(x), \tag{1}$$

where x is the input, m is the number of radial basis functions (neurons), $\{g^{(i)}\}_{i=1}^{m}$ is the set of RBFs and $\{w^{(i)}\}_{i=1}^{m}$ is the set of network weights to be found. Two radial basis functions of particular interest in the present study are

1. Multiquadrics (MQ)

$$g^{(i)}(x) = \sqrt{(x - c^{(i)})^2 + a^{(i)2}}, \tag{2}$$

2. Gaussian functions

$$g^{(i)}(x) = \exp\left(-\frac{(x - c^{(i)})^2}{a^{(i)2}}\right), \tag{3}$$

where $\{c^{(i)}\}_{i=1}^{m}$ is the set of RBF centres and $\{a^{(i)}\}_{i=1}^{m}$ is the set of RBF widths. In order to keep the design of RBFN simple (i.e. using only linear algebra), the centres and widths of the radial basis functions in the network (1) need be chosen in advance. In general the performance of RBFNs critically depend on these choices. Small or large values of the RBF width make the response of a neuron too peaked or too flat respectively and therefore should be avoided (Haykin [29]). In the present study, the width of the ith RBF is determined according to the following simple relation

$$a^{(i)} = \beta d^{(i)}, \tag{4}$$

where β is a factor, $\beta > 0$, and $d^{(i)}$ is the distance from the ith centre to the nearest centre. This relation (4) allows the RBF width a to be broader in the area of lower data density. By providing a set of the input $\{x^{(j)}\}_{j=1}^{n}$ where n is the number of collocation points and the corresponding desired output set $\{y^{(j)}\}_{j=1}^{n}$, the set of network weights $\{w^{(i)}\}_{i=1}^{m}$ can be found using the general linear least square methods.

2.1 Direct approach (DRBFN)

In the direct method, the closed form RBFN approximating function (1) is first obtained from a set of training points, and its derivative of any order, e.g. pth order, can then be calculated in a straightforward manner by differentiating such a closed form RBFN as follows

$$\frac{d^p f(x)}{dx^p} = \frac{d^p}{dx^p}\left(\sum_{i=1}^{m} w^{(i)} g^{(i)}(x)\right) = \sum_{i=1}^{m} w^{(i)}\left(\frac{d^p g^{(i)}(x)}{dx^p}\right) = \sum_{i=1}^{m} w^{(i)} h_{[p]}^{(i)}(x), \tag{5}$$

where $h_{[p]}^{(i)}$ denotes the pth order derivative of the radial basis function g. Once the set of network weights in (1) is obtained, the derivative (5) at any point is easily computed provided that new basis functions $\{h_{[p]}^{(i)}\}_{i=1}^{m}$ are given in analytic forms.

Since the direct approach is based on a differentiation process, all derivatives obtained here are very sensitive to noise arising from the interpolation of RBFNs from a set of discrete data points. Any noise here, even at the small level, will be badly magnified with an increase in the order of derivative. In contrast, the integration process, where each integral represents the area under the corresponding curve, is much less sensitive to noise. Based on this observation, it is expected that through the integration process, the approximating functions are much smoother and therefore have higher approximation power.

2.2 Indirect approach (IRBFN)

In the indirect method, the formulation of the problem starts with the decomposition of the highest order derivative under consideration into RBFs. The derivative expression obtained is then integrated to yield expressions for lower order derivatives and finally for the original function itself. The expression of the original function is employed in the general linear least square formulation for the unknown weights in a set of given discrete data points. Let p be the highest order of the derivative

under consideration, a part of the process above can be summarized as follows

$$\frac{d^p f(x)}{dx^p} = \sum_{i=1}^{m} w^{(i)} g^{(i)}(x), \tag{6}$$

$$\frac{d^{p-1} f(x)}{dx^{p-1}} = \int \sum_{i=1}^{m} w^{(i)} g^{(i)}(x) dx + c_1 = \sum_{i=1}^{m} w^{(i)} \int g^{(i)}(x) dx + c_1 = \sum_{i=1}^{m} w^{(i)} H_{[p-1]}^{(i)} + c_1$$

$$= \sum_{i=1}^{m+1} w^{(i)} H_{[p-1]}^{(i)}, \tag{7}$$

$$\frac{d^{p-2} f(x)}{dx^{p-2}} = \sum_{i=1}^{m} w^{(i)} \int H_{[p-1]}^{(i)} dx + c_1 x + c_2 = \sum_{i=1}^{m} w^{(i)} H_{[p-2]}^{(i)} + c_1 x + c_2$$

$$= \sum_{i=1}^{m+2} w^{(i)} H_{[p-2]}^{(i)}, \tag{8}$$

$$\cdots\cdots\cdots\cdots\cdots\cdots\cdots\cdots\cdots\cdots\cdots\cdots$$

$$\frac{df(x)}{dx} = \sum_{i=1}^{m} w^{(i)} \int H_{[2]}^{(i)} dx + c_1 \frac{x^{p-2}}{(p-2)!} + c_2 \frac{x^{p-3}}{(p-3)!} + \cdots + c_{p-2} x + c_{p-1}$$

$$= \sum_{i=1}^{m+p-1} w^{(i)} H_{[1]}^{(i)}, \tag{9}$$

$$f(x) = \sum_{i=1}^{m} w^{(i)} \int H_{[1]}^{(i)} dx + c_1 \frac{x^{p-1}}{(p-1)!} + c_2 \frac{x^{p-2}}{(p-2)!} + \cdots + c_{p-1} x + c_p$$

$$= \sum_{i=1}^{m+p} w^{(i)} H_{[0]}^{(i)}, \tag{10}$$

where $\{H_{[.]}^{(i)}\}_{i=1}^{m}$ are new basis functions obtained from integrating the radial basis function g. For convenience, integration constants which are unknowns here and their associated known basis functions (polynomial) on right hand sides in (6)-(10) are also denoted by the notations $w^{(i)}$ and $H_{[.]}^{(i)}$ respectively but with $i > m$.

For 2D or 3D problems, the integration constants c_i become functions and can be approximated by IRBFNs. The detailed implementation was reported previously in Mai-Duy and Tran-Cong [18].

3 BASIS FUNCTIONS

In an RBF collocation method, the original function and its derivatives are all expressed as linear combinations of basis functions, which are associated with the same set of network weights. In most cases, e.g. the direct approach with multiquadrics/Gaussian functions and the indirect approach with multiquadrics, expressions for new basis functions can be found analytically as shown in the appendix, which yield truly meshless methods. However, in some cases, analytic expressions are not available. For example, explicit integrals of Gaussian functions in (6)-(10) of the indirect approach can not be found and hence numerical integrations must be resorted to. The remainder of this section provides a numerical integration scheme for the purpose of obtaining these new basis functions. Let t be the variable, then the approximate function f together with its derivatives are expressed in terms of basis functions as

$$\begin{aligned}
\frac{d^p f(t)}{dt^p} &= \sum_{i=1}^{m} w^{(i)} g^{(i)}(t), && (11)\\
\frac{d^{p-1} f(x)}{dt^{p-1}} - \frac{d^{p-1} f(a)}{dt^{p-1}} &= \sum_{i=1}^{m} w^{(i)} \int_a^x g^{(i)}(t)dt, && (12)\\
\frac{d^{p-2} f(x)}{dt^{p-2}} - \frac{d^{p-2} f(a)}{dt^{p-2}} &= \sum_{i=1}^{m} w^{(i)} \int_a^x dt_2 \int_a^{t_2} g^{(i)}(t)dt, && (13)\\
&\cdots\cdots\cdots\\
\frac{df(x)}{dt} - \frac{df(a)}{dt} &= \sum_{i=1}^{m} w^{(i)} \int_a^x dt_{p-1} \ldots \int_a^{t_3} dt_2 \int_a^{t_2} g(t)dt, && (14)\\
f(x) - f(a) &= \sum_{i=1}^{m} w^{(i)} \int_a^x dt_p \int_a^{t_p} dt_{k-1} \ldots \int_a^{t_3} dt_2 \int_a^{t_2} g(t)dt, && (15)
\end{aligned}$$

where a and x are two reference collocation points. Fortunately, integrals on right hand sides over the finite interval between a and x can be reduced to one dimensional integrals by using the formula of iterated integrals (Abramowitz and Stegun [30]),

e.g.

$$\int_a^x dt_k \int_a^{t_k} dt_{k-1} \ldots \int_a^{t_3} dt_2 \int_a^{t_2} g(t)dt = \frac{(x-a)^k}{(k-1)!} \int_0^1 t^{k-1} g(x-(x-a)t)dt. \quad (16)$$

for which Gaussian quadrature can now be applied. Some background mesh is thus necessary for the indirect approach with the use of Gaussian functions.

4 NUMERICAL SOLUTION OF ODES

In the case of traditional numerical methods, it is known that the boundary value problems can require considerably more effort to solve than the initial value problems. However, in the present case, the unsymmetric RBF collocation methods work in a similar fashion for both problems and they are quite simple as illustrated here on the initial-value problem governed by the following pth order ODE

$$y^{[p]} = F(x, y, y', \ldots, y^{[p-1]}) \quad (17)$$

with initial conditions

$$y(a) = \alpha_1,\ y'(a) = \alpha_2,\ \ldots,\ y^{[p-1]}(a) = \alpha_p, \quad (18)$$

where $a \leq x \leq b$, $y^{[i]}(x) = \frac{d^i y(x)}{dx^i}$, F is a known function and $\{\alpha_i\}_{i=1}^p$ is a set of prescribed conditions. In solving (17)-(18), for both direct and indirect approaches, the interior collocation points are enforced to satisfy the governing ODEs while the boundary collocation points are employed to satisfy not only the boundary conditions but also the governing ODEs, resulting in the following sum of squared

errors

$$\sum_{j=1}^{n}\left[\sum_{i=1}^{m} w^{(i)} h_{[p]}^{(i)}(x^{(j)}) - F\left(x^{(j)}, \sum_{i=1}^{m} w^{(i)} g^{(i)}(x^{(j)}), \sum_{i=1}^{m} w^{(i)} h_{[1]}^{(i)}(x^{(j)}), \ldots, \sum_{i=1}^{m} w^{(i)} h_{[p-1]}^{(i)}(x^{(j)})\right)\right]^2$$
$$+ \left[\sum_{i=1}^{m} w^{(i)} g^{(i)}(a) - \alpha_1\right]^2 + \left[\sum_{i=1}^{m} w^{(i)} h_{[1]}^{(i)}(a) - \alpha_2\right]^2 + \ldots + \left[\sum_{i=1}^{m} w^{(i)} h_{[p-1]}^{(i)}(a) - \alpha_p\right]^2 \to 0 \tag{19}$$

for the direct approach and

$$\sum_{j=1}^{n}\left[\sum_{i=1}^{m} w^{(i)} g^{(i)}(x^{(j)}) - F\left(x^{(j)}, \sum_{i=1}^{m+p} w^{(i)} H_{[0]}^{(i)}(x^{(j)}), \sum_{i=1}^{m+p-1} w^{(i)} H_{[1]}^{(i)}(x^{(j)}), \ldots, \sum_{i=1}^{m+1} w^{(i)} H_{[p-1]}^{(i)}(x^{(j)})\right)\right]^2$$
$$+ \left[\sum_{i=1}^{m+p} w^{(i)} H_{[0]}^{(i)}(a) - \alpha_1\right]^2 + \left[\sum_{i=1}^{m+p-1} w^{(i)} H_{[1]}^{(i)}(a) - \alpha_2\right]^2 + \ldots + \left[\sum_{i=1}^{m+1} w^{(i)} H_{[p-1]}^{(i)}(a) - \alpha_p\right]^2 \to 0 \tag{20}$$

for the indirect approach, in which m is the number of centres (RBFs) and n is the number of collocation points. From a neural network approximation point of view, the system of equations obtained directly from (19) or (20) can be square or non-square depending on the number of centres m and the number of collocation points n to be used. The former decides the number of columns of the design matrix while the latter determines the number of rows. In the field of numerical solution of differential equations, the set of collocation points is widely chosen to be the same as the set of centres. As a result, the obtained system is overdetermined for the direct approach, even for the case that the governing ODE (17) is applied to the interior collocation points only (not to the boundary collocation points as stated above). However, for the indirect approach, owing to the appearance of integration constants whose number is equal to the order of ODE, the system obtained is always determined, irrespective of the order of ODE. This is a clear advantage of the indirect approach over the direct approach in the treatment of multiple boundary conditions. For other numerical methods, to implement multiple boundary conditions at a point,

some special techniques are normally required. For example, in the DQ method (e.g. Gutierrez and Laura [6]), some points adjacent to the boundaries are introduced and enforced to act as boundary points ($\delta-$point technique) or in the Generalized Differential Quadrature Rule (GDQR) (e.g. Wu and Liu [7,8,9]), the derivatives at boundary points are also regarded as independent variables.

After solving (19) by the general least squares or (20) by Gaussian elimination, the set of network weights is obtained and hence the dependent variable together with its derivatives at any point will be computed easily.

There are some reasons that multiquadrics (MQ) are recommended for practical use. Firstly, the MQ function yields greater accuracy than other RBFs in approximating a smooth input-output mapping (Haykin [29]). Secondly, it has exponential convergence with the refinement of spatial discretization (Madych and Nelson, [31,32]) and thirdly, for the indirect approach, the need for the element-based discretization of the domain is completely eliminated here (truly meshless method). In the remainder of this paper, for both unsymmetric direct and indirect collocation approaches, only multiquadrics are considered.

5 NUMERICAL EXAMPLES

In the following examples, the set of collocation points is chosen to be the same as the set of centres, i.e. $\{c^{(i)}\}_{i=1}^{m} = \{x^{(i)}\}_{i=1}^{m}$. The accuracy of numerical solution produced by an approximation scheme is measured via the norm of relative errors of the solution as follows

$$N_e = \sqrt{\frac{\sum_{i=1}^{n_t} \left[y(x^{(i)}) - f(x^{(i)})\right]^2}{\sum_{i=1}^{n_t} y(x^{(i)})^2}}, \tag{21}$$

where n_t is the number of test points, $x^{(i)}$ is the ith test point, f and y are the calculated and exact functions respectively. Another important measure is the convergence rate of the solution with the refinement of spatial discretization

$$N_e(h) \approx \gamma h^{\alpha} = O(h^{\alpha}) \tag{22}$$

in which h is the centre spacing, and α and γ are the exponential model's parameters. Given a set of observations, these parameters can be found by the general linear least squares.

5.1 High order derivatives

Consider the following function of one variable

$$y = \sin(x), \tag{23}$$

with $0 \leq x \leq 2\pi$. The derivative of any order of function (23) can be found analytically without difficulty. A wide range of the order of derivative from 1 to 8 is considered here. Two data sets of 21 and 101 points with uniform distributions are employed for training and testing respectively. The global error of the computed solution is measured through the norm of relative errors of the solution at test points as defined in (21). Results of Ne obtained by two approaches using the same network parameters ($\beta = 1,\ n = m = 21,\ n_t = 101$) are displayed in Figure 1, which show that the performance of the indirect approach is clearly superior to that of the direct approach on both function and derivative approximations. For both approaches, the error norm is an increasing function of the order of derivative. Some plots of derivatives are displayed in Figure 2, which indicates that the direct approach fails to capture the solution when the order of derivative is greater than 2

while the indirect approach is able to capture all the derivative functions. For low orders, there is no discernible difference between the IRBF and the exact solutions (Figure 2).

In the case of the indirect approach, two aspects are further studied here. Firstly, how does the "order" of the IRBFN scheme affect the accuracy of numerical solution. The ith order IRBFN scheme, IRBFN-i, is regarded as an indirect scheme in which the ith order derivative is decomposed into a set of RBFs. There are two concepts of the order used throughout the present study, namely the order of derivative/ODE and the order of an IRBFN scheme. To represent an ith order derivative, the indirect scheme needs be employed with at least ith order. Increasing the order of IRBFN can improve the solution accuracy as shown in Figure 3. Secondly, the effect of β on the solution accuracy is also investigated. It is known that large or small values of the RBF width make the response of the corresponding basis function too flat or too peaked respectively and therefore both of these two extreme conditions should be avoided (Haykin [29]). Figure 4 shows that better approximations are obtained with an increase in β up to the value of about 7.

The approximation of 6th order derivative of function (23) is reconsidered. By increasing

- the value of β up to 7, or
- the order of IRBFN up to 10, or
- a number of centres up to 41,

the obtained solution is improved as displayed in Figure 5. The corresponding error-nomrs are reduced from 0.0245 (IRBFN-8, $\beta = 1$) to 0.0030 (IRBFN-8, $\beta = 7$), 0.0022 (IRBFN-10, $\beta = 1$) and 0.0033 (IRBFN-8, $\beta = 1, n = 41$).

5.2 High order ODEs

The theoretical determinant for the optimum value of the RBF width has not been established yet. For the approximation of a function and its derivatives, the numerical example above indicated that the indirect approach performs well for a wide range of β. In solving second order DEs (Mai-Duy and Tran-Cong [16]), experience showed that the value of β can be chosen in the range $1 \leq \beta \leq 10$. In the present study, all values of β are simply fixed to be 7. Furthermore, the order of IRBFN is chosen to be the same as that of ODE. In the indirect approach, Gaussian elimination is applied to solve the systems of equations because all design matrices obtained here are square. In the direct approach, the design matrices are non-square so that the corresponding systems are solved in the least square sense unless otherwise stated.

5.2.1 Fourth order ODE - Boundary value problem

The problem here is to find a function $y(x)$ satisfying the following fourth order ODE

$$x^4 y^{[4]} - 4x^3 y''' + x^2(12 - x^2)y'' + 2x(x^2 - 12)y' + 2(12 - x^2)y = 2x^5, \qquad (24)$$

over a specified interval of the x axis, $1 \leq x \leq 11$, subject to the boundary conditions for y and y' at both ends of the domain. Note that this is a nonhomogeneous ODE with coefficients being functions of x. The exact solution of (24) can be verified to be

$$y = x + x^2 - x^3 + x\exp(x) + x\exp(-x).$$

To study convergence, four sets of 6, 11, 17 and 21 equally spaced points ($m = n = \{6, 11, 17, 21\}$) are employed for the design of networks in both DRBF and IRBF collocation procedures. The governing equation (24) and boundary conditions are

transformed into

$$x^4 \sum_{i=1}^{m} w^{(i)} h_{[4]}^{(i)}(x) - 4x^3 \sum_{i=1}^{m} w^{(i)} h_{[3]}^{(i)}(x) + x^2(12 - x^2) \sum_{i=1}^{m} w^{(i)} h_{[2]}^{(i)}(x) + 2x(x^2 - 12) \sum_{i=1}^{m} w^{(i)} h_{[1]}^{(i)}(x) + 2(12 - x^2) \sum_{i=1}^{m} w^{(i)} g^{(i)}(x) = 2x^5, \quad (25)$$

$$\sum_{i=1}^{m} w^{(i)} g^{(i)}(1) = 1 + \exp(1) + \exp(-1), \quad (26)$$

$$\sum_{i=1}^{m} w^{(i)} h_{[1]}^{(i)}(1) = 2\exp(1), \quad (27)$$

$$\sum_{i=1}^{m} w^{(i)} g^{(i)}(11) = 11 + 11^2 - 11^3 + 11\exp(11) + 11\exp(-11), \quad (28)$$

$$\sum_{i=1}^{m} w^{(i)} h_{[1]}^{(i)}(11) = 1 + 2(11) - 3(11)^2 + 12\exp(11) - 10\exp(-11), \quad (29)$$

for the direct approach and

$$x^4 \sum_{i=1}^{m} w^{(i)} g^{(i)}(x) - 4x^3 \sum_{i=1}^{m+1} w^{(i)} H_{[3]}^{(i)}(x) + x^2(12 - x^2) \sum_{i=1}^{m+2} w^{(i)} H_{[2]}^{(i)}(x) + 2x(x^2 - 12) \sum_{i=1}^{m+3} w^{(i)} H_{[1]}^{(i)}(x) + 2(12 - x^2) \sum_{i=1}^{m+4} w^{(i)} H_{[0]}^{(i)}(x) = 2x^5, \quad (30)$$

$$\sum_{i=1}^{m+4} w^{(i)} H_{[0]}^{(i)}(1) = 1 + \exp(1) + \exp(-1), \quad (31)$$

$$\sum_{i=1}^{m+3} w^{(i)} H_{[1]}^{(i)}(1) = 2\exp(1), \quad (32)$$

$$\sum_{i=1}^{m+4} w^{(i)} H_{[0]}^{(i)}(11) = 11 + 11^2 - 11^3 + 11\exp(11) + 11\exp(-11), \quad (33)$$

$$\sum_{i=1}^{m+3} w^{(i)} H_{[1]}^{(i)}(11) = 1 + 2(11) - 3(11)^2 + 12\exp(11) - 10\exp(-11), \quad (34)$$

for the indirect approach, in which the unknowns are network weights $\{w^{(i)}\}$. The evaluation of (25) or (30) at a set of collocation points $\{x^{(i)}\}_{i=1}^{n}$ plus the discretization of boundary conditions (26)-(29) or (31)-(34) results in the system of equations of

the form

$$\mathbf{A}\mathbf{w} = \mathbf{b},$$

where $\mathbf{A}$ is an $(n+4) - \text{by} - m$ matrix for the direct approach and an $(n+4) - \text{by} - (m+4)$ matrix for the indirect approach. For all study cases, error norms of the solution y are calculated at a test set of 101 uniformly distributed points. Figure 6 shows that the indirect approach yields very accurate results and also a high convergence rate while the opposite is true for the direct approach. Solutions converge apparently as $O(h^{-0.0447})$ and $O(h^{7.1594})$ with h being the centre spacing for the direct and indirect approaches respectively. At the finest discretization used here (i.e. 21 training data points), error norms of the solution are 2.48 and $1.23e-6$ for the direct and indirect approaches respectively.

It can be seen from Figure 6 that the performance of the direct approach is very poor, for example, no "mesh" convergence is observed there. As discussed above, the obtained system is overdetermined for the direct approach, but determined for the indirect approach. The question here is whether the performance of the direct approach can be improved when its design matrices are square. To make the matrix of the direct approach square, the following relation needs be satisfied

$$n + p = m, \tag{35}$$

where p is the order of ODE. In other words, the number of collocation points used to approximate the strong form of the governing equation must be chosen less than the number of centres (i.e. $n < m$). For the problem under consideration here, by not applying the ODE at two boundary points together with two interior points (for example, interior points adjacent to the boundaries are set aside here), the relation (35) is satisfied and Gaussian elimination can be applied to solve the final systems of equations. Results obtained are improved as displayed in Figurre 6,

where the convergence rate is of $O(h^{2.1744})$ (h is the centre spacing) and the error norm is 0.0591 at the finest discretization. However, they are still far less accurate than those obtained by the proposed indirect approach and also have much lower convergence rate.

5.2.2 Fourth order ODE - Eigenvalue problem

Consider the transverse vibration of an uniform beam of length l for which the general equation takes the form

$$\frac{\partial^4 y}{\partial x^4} + \left(\frac{\rho A}{EI}\right)\frac{\partial^2 y}{\partial t^2} = 0, \tag{36}$$

where ρ, E and I are the mass per unit length, the elastic module and the area moment of inertia about the neutral axis respectively. Assuming that the deflection at any point of the beam varies harmonically with time

$$y(x,t) = \phi(x)sin(\omega t). \tag{37}$$

Substitution of (37) into (36) yields

$$\frac{\partial^4 \phi}{\partial x^4} - \lambda^4 \phi = 0, \tag{38}$$

where $\lambda^4 = \rho A\omega^2/EI$. The following are three types of boundary condition to be considered here

- Pinned-pinned beam

$$\phi(0) = \phi''(0) = 0, \quad \phi(l) = \phi''(l) = 0; \tag{39}$$

- Clamped-clamped beam

$$\phi(0) = \phi'(0) = 0, \quad \phi(l) = \phi'(l) = 0; \tag{40}$$

- Clamped-pinned beam

$$\phi(0) = \phi'(0) = 0, \quad \phi(l) = \phi''(l) = 0. \tag{41}$$

Eigenvalue problems require more effort to form the final system of equations than boundary value problems. Substitution of the closed form IRBFN representations of the variable ϕ and its derivatives (6)-(10) into the governing equation (38) and also boundary conditions, e.g. (39) for the case of pinned-pinned beam, yields

$$\sum_{i=1}^{m} w^{(i)} g^{(i)}(x) - \lambda^4 \sum_{i=1}^{m+4} w^{(i)} H_{[0]}^{(i)}(x) = 0, \tag{42}$$

$$\sum_{i=1}^{m+4} w^{(i)} H_{[0]}^{(i)}(0) = 0, \tag{43}$$

$$\sum_{i=1}^{m+2} w^{(i)} H_{[2]}^{(i)}(0) = 0, \tag{44}$$

$$\sum_{i=1}^{m+4} w^{(i)} H_{[0]}^{(i)}(l) = 0, \tag{45}$$

$$\sum_{i=1}^{m+2} w^{(i)} H_{[2]}^{(i)}(l) = 0, \tag{46}$$

or in the matrix form,

$$\mathbf{A}\mathbf{w} - \lambda^4 \mathbf{B}\mathbf{w} = \mathbf{0}, \tag{47}$$

$$\mathbf{C}\mathbf{w} = \mathbf{0}, \tag{48}$$

or

$$(\mathbf{A}_1, \mathbf{A}_2)(\mathbf{w}_1, \mathbf{w}_2)^T - \lambda^4(\mathbf{B}_1, \mathbf{B}_2)(\mathbf{w}_1, \mathbf{w}_2)^T = \mathbf{0}, \quad (49)$$

$$(\mathbf{C}_1, \mathbf{C}_2)(\mathbf{w}_1, \mathbf{w}_2)^T = \mathbf{0}, \quad (50)$$

where the dimensions of submatrices are $n \times n(\mathbf{A}_1)$, $n \times p(\mathbf{A}_2)$, $n \times n(\mathbf{B}_1)$, $n \times p(\mathbf{B}_2)$, $p \times n(\mathbf{C}_1)$, $p \times p(\mathbf{C}_2)$, $1 \times n(\mathbf{w}_1)$ and $1 \times p(\mathbf{w}_2)$ in which n and p are the number of collocation points (centres) and the order of ODE respectively ($p = 4$ here). With some manipulations on (49) and (50), the final system of equations takes the form

$$[(\mathbf{A}_1 - \mathbf{A}_2\mathbf{C}_2^{-1}\mathbf{C}_1) - \lambda^4(\mathbf{B}_1 - \mathbf{B}_2\mathbf{C}_2^{-1}\mathbf{C}_1)]\mathbf{w}_1^T = \mathbf{0}. \quad (51)$$

Results of λ obtained with $l = 1$ are displayed in Tables 1, 2 and 3 for pinned-pinned, clamped-clamped and clamped-pinned beams respectively. The analytic solution is also given for comparison. The proposed method achieves accurate results and also high rates of convergence for all study cases.

It is observed that when increasing data densities, the computed results are consistently more accurate, but their values slightly oscillate about the exact values, e.g. the case: λ_4, pinned-pinned beam (Table 1). The reason for this behaviour is not clear, probably due to the combined effect of the centre density and the value of β.

5.2.3 Sixth order ODE - Vibrations of ring-like structures

The vibrational behaviour of ring-like structures, which is important in engineering applications, is considered in this section. The vibration problem governed by the sixth order differential equation was studied by Gutierrez and Laura [6] using the differential quadrature method (DQM) and the optimized Rayleigh-Ritz method and by Wu and Liu [7] using the generalized differential quadrature rule (GDQR).

The structural element is a ring of rectangular cross-section of constant width and thickness which varies parabolically according to the relation (Figure 7):

$$h(\bar{\alpha}) = h(0)\left[-\frac{4}{\pi^2}(r-1)\bar{\alpha}^2 + \frac{4}{\pi}(r-1)\bar{\alpha} + 1\right] = h(0)f(\bar{\alpha}), \tag{52}$$

where $r = h(\pi/2)/h(0)$. The case of normal, in-plane modes of vibration is studied here, where only flexural effects are taken into account and one disregards stretching in the axial direction.

A circular ring with supports (Figure 7-a): Since the structure is symmetric, only half of the domain is considered. Introducing the dimensionless variable $\alpha = \bar{\alpha}/\pi$, the governing differential equation can be expressed in the form

$$\beta_1 v^{[6]} + \beta_2 v^{[5]} + \beta_3 v^{[4]} + \beta_4 v^{'''} + \beta_5 v^{''} + \beta_6 v^{'} - \Omega^2\left(fv^{''} + f^{'}v^{'} - \pi^2 fv\right) = 0, \tag{53}$$

subject to the boundary conditions

$$v(0) = v^{'}(0) = v^{'''}(0) = 0, \quad v(1) = v^{'}(1) = v^{'''}(1) = 0,$$

where v is the tangential displacement, Ω is the dimensionless frequency and

$$\begin{aligned}
0 &\leq \alpha \leq 1 \\
\beta_1 &= \phi/\pi^4, \quad \beta_2 = 3\phi^{'}/\pi^4, \quad \beta_3 = (2\phi/\pi^2) + (3\phi^{''}/\pi^4), \\
\beta_4 &= (4\phi^{'}/\pi^2) + (\phi^{'''}/\pi^4), \quad \beta_5 = \phi + (3\phi^{''}/\pi^2), \quad \beta_6 = \phi^{'} + (\phi^{'''}/\pi^2), \\
\phi &= [f(\alpha)]^3.
\end{aligned}$$

The solution procedures are similar to the problem of transverse vibration of a beam in the previous section and therefore omitted here for brevity. Five data sets of 6, 7, 8, 9 and 10 uniformly distributed points are employed. The fundamental frequency

coefficients of in-plane, inextensional vibration obtained are listed in Table 4. The values predicted by the DQM, the optimized Rayleigh-Ritz method and the GDQR method are also given for comparison purpose. Good agreements are observed. Both GDQR and IRBF collocation methods yield good results even if only 8 points are used for $r < 1.4$. For the DQM, it was found necessary to take $n = 12$ for $r = \{1.0; 1.1; 1.2; 1.3\}$ and $n = 14$ for $r = \{1.4; 1.5\}$ (Gutierrez and Laura [6]).

A completely free ring (Figure 7-b): In this case, a quarter of the ring structure is considered. It is convenient to introduce the dimensionless variable $\alpha = 2\bar{\alpha}/\pi$ here and the governing equations can be written as

$$\beta_1 v^{[6]} + \beta_2 v^{[5]} + \beta_3 v^{[4]} + \beta_4 v^{'''} + \beta_5 v^{''} + \beta_6 v^{'} - \Omega^2 \left(f v^{''} + f^{'} v^{'} - \pi^2 f v/4 \right) = 0, \quad (54)$$

subject to the boundary conditions

$$\begin{aligned} v(0) &= v^{''}(0) = 0, \quad \phi^{'}(0) \left[v^{'}(0) + 4 v^{'''}(0)/\pi^2 \right] + 4\phi(0) v^{[4]}(0)/\pi^2 = 0, \\ v(1) &= v^{''}(1) = 0, \quad \phi^{'}(1) \left[v^{'}(1) + 4 v^{'''}(1)/\pi^2 \right] + 4\phi(1) v^{[4]}(1)/\pi^2 = 0, \end{aligned}$$

where

$$\begin{aligned} 0 &\leq \alpha \leq 1 \\ \beta_1 &= 16\phi/\pi^4, \quad \beta_2 = 48\phi^{'}/\pi^4, \quad \beta_3 = (8\phi/\pi^2) + (48\phi^{''}/\pi^4), \\ \beta_4 &= (16\phi^{'}/\pi^2) + (16\phi^{'''}/\pi^4), \quad \beta_5 = \phi + (12\phi^{''}/\pi^2), \quad \beta_6 = \phi^{'} + (4\phi^{'''}/\pi^2), \\ \phi &= [f(\alpha)]^3. \end{aligned}$$

Table 5 displays the results obtained by the present method together with those obtained by the DQM, GDQR and Rayleigh-Ritz methods. Values differ only in the third or fourth significant digit so all solutions are reasonable approximations. With the use of 6 data points only, good results are obtained with the GDQR and

IRBF collocation methods. Note that the DQM was reported to use 12 data points for this case.

5.2.4 Eighth order ODE - Initial value problem and boundary value problem

The unsymmetric IRBF collocation method is further verified here in the solution of eighth order ODE

$$y^{[8]} + y^{[7]} + y^{[6]} + y^{[5]} + y^{[4]} + y''' + y'' + y' + y = 9\exp(x), \tag{55}$$

over the interval $0 \leq x \leq 1$.

Firstly, the initial value problem governed by (55) with initial values

$$y(0) = y'(0) = y''(0) = y'''(0) = y^{[4]}(0) = y^{[5]}(0) = y^{[6]}(0) = y^{[7]}(0) = 1, \tag{56}$$

is considered. The exact solution of (55) and (56) can be verified to be $y(x) = \exp(x)$. A number of uniform data sets whose sizes vary from 3 to 6 with an increment of 1 are chosen to be the sets of centres. For comparison purpose, the fourth order Runge-Kutta method is also applied here to solve this problem using the same data sets, in which the centre spacing is interpreted as time step. Good accuracy and high rate of convergence are obtained for both methods especially for the proposed method (Figure 8). Solutions converge apparently as $O(h^{3.8408})$ and $O(h^{5.8484})$ with h being the centre spacing for the Runge-Kutta and IRBF collocation methods respectively. The present method achieves error-norms at least three order lower than the Runge-Kutta method. For example, at the centre spacing of $1/5$, error-norms are $8.70e-6$ and $1.76e-10$ for the traditional and proposed methods respectively.

Secondly, the boundary value problem governed by the eighth order ODE above is considered. Four boundary conditions for y, y', y'' and $y^{[3]}$ whose values are computed from the exact solution $y(x) = \exp(x)$ are imposed at both-ends of the domain. Five data densities of 5, 6, 7, 8 and 9 equally spaced points together with 101 test points are employed to investigate this problem. The proposed method yields very good results for all densities with the corresponding error-norms being $4.48e-13, 9.34e-14, 1.54e-14, 4.70e-15$ and $1.32e-15$ respectively. Figure 9 shows that a high convergence rate up to $O(h^{8.4703})$ (h is the centre spacing) is achieved with the present method.

5.2.5 Eighth order ODE - Simply supported single-barrel shell with free edges

This problem is taken from reference (Kelkar and Sewell [33]) and was studied by Wu and Liu [9] using the GDQR (Figure 10). The shell parameters are a longitudinal length of $L = 42$ ft, a barrel radius of $a = 12.5$ ft and a shell thickness of $t = 0.25$ ft. The half angle of the barrel is 40^o. The circular cylindrical single-barrel roof is free at the two edges along the longitudinal x-direction with $0 \leq x \leq L$ and simply supported at the other two circular edges $x = 0$ and $x = L$. An equivalent dead distributed load of $p = 62.5$ lb/ft^2 is considered. Since the L/a ratio is greater than 3, the Schorer theory can be applied to solve this problem. The shell only for the first harmonic of the Fourier series expansion for the loading is analyzed here. The radial displacement is thus expressed as follows

$$v(x, \phi) = V(\phi) \sin \frac{\pi x}{L}. \tag{57}$$

The analysis of Kelkar and Sewell [33] leads to the following governing eighth order ODE

$$V^{[8]} + \lambda^8 V = -\frac{-8pa^4 \cos\phi}{\pi K}, \tag{58}$$

subject to the four boundary conditions for stress at free edges as follows

$$M_\phi = 0, \quad Q_\phi = 0, \quad N_\phi = 0 \quad \text{and} \quad N_{x\phi} = 0, \tag{59}$$

where $\lambda^8 = 12\pi^4 a^6/(L^4 t^2)$, $K = Et^3/12$ and E is the Young's modulus.

The solution V can be decomposed into a homogeneous part V^h and a particular solution part V^p as

$$V = V^h + V^p.$$

The membrane solution is adopted as the particular solution whose form for some bending stresses of particular interest here is

$$\begin{aligned}
M_\phi^p &= 0, && (60)\\
Q_\phi^p &= 0, && (61)\\
N_\phi^p &= -\frac{4pa}{\pi}\cos\phi \sin\frac{\pi x}{L}, && (62)\\
N_{x\phi}^p &= \frac{8pL}{\pi^2}\sin\phi\cos\frac{\pi x}{L}, && (63)\\
N_x^p &= -\frac{8pL^2}{\pi^3 a}\cos\phi\sin\frac{\pi x}{L}. && (64)
\end{aligned}$$

With loads taken as zero for the homogeneous solution, expressions for the stress

resultants are given by

$$M_{\phi}^{h} = \frac{K}{a^2}\frac{d^2V}{d\phi^2}\sin\frac{\pi x}{L}, \tag{65}$$

$$Q_{\phi}^{h} = \frac{K}{a^3}\frac{d^3V}{d\phi^3}\sin\frac{\pi x}{L}, \tag{66}$$

$$N_{\phi}^{h} = -\frac{K}{a^3}\frac{d^4V}{d\phi^4}\sin\frac{\pi x}{L}, \tag{67}$$

$$N_{x\phi}^{h} = -\frac{KL}{\pi a^4}\frac{d^5V}{d\phi^5}\cos\frac{\pi x}{L}, \tag{68}$$

$$N_{x}^{h} = \frac{KL^2}{\pi^2 a^5}\frac{d^6V}{d\phi^6}\sin\frac{\pi x}{L}, \tag{69}$$

The task now is to find the solution of the homogeneous governing equation corresponding to (58)

$$V^{h[8]} + \lambda^8 V^h = 0, \tag{70}$$

subject to the four boundary conditions at each edge

$$M_{\phi}^{h} = -M_{\phi}^{p}, \quad Q_{\phi}^{h} = -Q_{\phi}^{p}, \quad N_{\phi}^{h} = -N_{\phi}^{p} \quad \text{and} \quad N_{x\phi}^{h} = -N_{x\phi}^{p},$$

or

$$\frac{d^2V^h}{d\phi^2} = 0, \quad \frac{d^3V^h}{d\phi^3} = 0, \quad \frac{d^4V^h}{d\phi^4} = -\frac{4pa^4}{\pi K}\cos\phi, \quad \text{and} \quad \frac{d^5V^h}{d\phi^5} = \frac{8pa^4}{\pi K}\sin\phi. \tag{71}$$

The unsymmetric IRBF collocation procedure to solve (70)-(71) is similar to the previous numerical examples. Results obtained (V^h and its derivatives) are then substituted into (65)-(69) to produce the force and moment resultants. The analytic homogeneous results can be found in (Kelkar and Sewell [33]) and (Wu and Liu [9]). Note that the coefficients of the analytic results provided in (Kelkar and Sewell [33]) are only accurate to two significant figures. To obtain higher accuracy, Wu and Liu [9] recalculated those values. The analytic homogeneous results of Wu and Liu [9] are

used here for comparison. Tables 6-8 present the final computed force and moment resultants using 5, 9 and 13 equally spaced points. With only a few equally spaced points, the IRBF results are in very good agreement with the analytic results. It also shows that the finer density yields a better approximation to the true value. The difference is less than 0.085 % in all cases. At the finest data density ($n = 13$), the maximum error is 0.00004%. It is remarkable because the computed stress resultants here involve derivatives up to 7th order. For the GDQR method, the cosine-type of the sampling points is employed. With the same numbers of data points used (i.e. 5, 9 and 13 points), the maximum error of the force and moment resultants is about 0.62% (Wu and Liu [9]), which is slightly greater than that obtained by the present method (0.085%).

6 CONCLUDING REMARKS

This paper reports new meshless numerical methods based on RBFNs for solving high order ODEs directly. Two unsymmetric RBF collocation approaches are employed to approximate the strong form of the governing equations and the boundary conditions. Like other meshless numerical methods (e.g. smoothed particle hydrodynamics, the vortex method, the generalized finite difference method and many others), the direct RBF collocation approach here is based on the differential process to represent the solution. By contrast, in the proposed indirect RBF collocation approach, the closed forms representing the dependent variable and its derivatives are obtained through the integration process. The use of the integration process results in higher approximation power for RBFNs. Furthermore, in the case of solving high order ODEs, the well-known difficulties to deal with multiple boundary conditions are naturally overcome via means of integration constants. Two present approaches are easy to implement and work in a similar fashion for both boundary

and initial value problems. It requires no extra effort when increasing the order of ODE. Analytic and numerical techniques for obtaining new basis functions from RBFs are discussed. Among RBFs, multiquadrics are preferred for practical use. Numerical results show that the proposed indirect approach performs much better than the usual direct approach. High convergence rates and good accuracy are obtained with the proposed method using relatively low numbers of data points. The proposed unsymmetric IRBF collocation method can be extended to the solution of high order PDEs which will be carried out in future work.

APPENDIX

The following are new basis functions derived from RBFs by using MATHEMATICA.

Direct approach - Multiquadrics

$$
\begin{aligned}
h^{(i)}_{[1]} &= \frac{x-c^{(i)}}{\left[(x-c^{(i)})^2+a^{(i)2}\right]^{1/2}},\\
h^{(i)}_{[2]} &= \frac{a^{(i)2}}{\left[(x-c^{(i)})^2+a^{(i)2}\right]^{3/2}},\\
h^{(i)}_{[3]} &= \frac{-3a^{(i)2}(x-c^{(i)})}{\left[(x-c^{(i)})^2+a^{(i)2}\right]^{5/2}},\\
h^{(i)}_{[4]} &= \frac{3a^{(i)2}\left[4(x-c^{(i)})^2-a^{(i)2}\right]}{\left[(x-c^{(i)})^2+a^{(i)2}\right]^{7/2}},\\
h^{(i)}_{[5]} &= \frac{-15a^{(i)2}(x-c^{(i)})\left[4(x-c^{(i)})^2-3a^{(i)2}\right]}{\left[(x-c^{(i)})^2+a^{(i)2}\right]^{9/2}},\\
h^{(i)}_{[6]} &= \frac{45a^{(i)2}\left[8(x-c^{(i)})^4-12a^{(i)2}(x-c^{(i)})^2+a^{(i)4}\right]}{\left[(x-c^{(i)})^2+a^{(i)2}\right]^{11/2}}\\
h^{(i)}_{[7]} &= \frac{-315a^{(i)2}(x-c^{(i)})\left[8(x-c^{(i)})^4-20a^{(i)2}(x-c^{(i)})^2+5a^{(i)4}\right]}{\left[(x-c^{(i)})^2+a^{(i)2}\right]^{13/2}},\\
h^{(i)}_{[8]} &= \frac{315a^{(i)2}\left[64(x-c^{(i)})^6-240a^{(i)2}(x-c^{(i)})^4+120a^{(i)4}(x-c^{(i)})^2-5a^{(i)6}\right]}{\left[(x-c^{(i)})^2+a^{(i)2}\right]^{15/2}}.
\end{aligned}
$$

Direct approach - Gaussians

$$
\begin{aligned}
h^{(i)}_{[1]} &= \frac{-2(x-c^{(i)})}{a^{(i)2}}\exp\left(-\frac{(x-c^{(i)})^2}{a^{(i)2}}\right),\\
h^{(i)}_{[2]} &= \frac{2\left[2(x-c^{(i)})^2-a^{(i)2}\right]}{a^{(i)4}}\exp\left(-\frac{(x-c^{(i)})^2}{a^{(i)2}}\right),\\
h^{(i)}_{[3]} &= \frac{-4(x-c^{(i)})\left[2(x-c^{(i)})^2-3a^{(i)2}\right]}{a^{(i)6}}\exp\left(-\frac{(x-c^{(i)})^2}{a^{(i)2}}\right),\\
h^{(i)}_{[4]} &= \frac{4\left[4(x-c^{(i)})^4-12(x-c^{(i)})^2a^{(i)2}+3a^{(i)4}\right]}{a^{(i)8}}\exp\left(-\frac{(x-c^{(i)})^2}{a^{(i)2}}\right),\\
h^{(i)}_{[5]} &= \frac{-8(x-c^{(i)})\left[4(x-c^{(i)})^4-20(x-c^{(i)})^2a^{(i)2}+15a^{(i)4}\right]}{a^{(i)10}}\exp\left(-\frac{(x-c^{(i)})^2}{a^{(i)2}}\right),\\
h^{(i)}_{[6]} &= \frac{8\left[8(x-c^{(i)})^6-60(x-c^{(i)})^4a^{(i)2}+90(x-c^{(i)})^2a^{(i)4}-15a^{(i)6}\right]}{a^{(i)12}}\exp\left(-\frac{(x-c^{(i)})^2}{a^{(i)2}}\right),\\
h^{(i)}_{[7]} &= \frac{-16(x-c^{(i)})\left[8(x-c^{(i)})^6-84(x-c^{(i)})^4a^{(i)2}+210(x-c^{(i)})^2a^{(i)4}-105a^{(i)6}\right]}{a^{(i)14}}\exp\left(-\frac{(x-c^{(i)})^2}{a^{(i)2}}\right),\\
h^{(i)}_{[8]} &= \frac{16\left[16(x-c^{(i)})^8-224(x-c^{(i)})^6a^{(i)2}+840(x-c^{(i)})^4a^{(i)4}-840(x-c^{(i)})^2a^{(i)6}+105a^{(i)8}\right]}{a^{(i)16}}\exp\left(-\frac{(x-c^{(i)})^2}{a^{(i)2}}\right).
\end{aligned}
$$

Indirect approach - Multiquadrics

$$
\begin{aligned}
H^{(i)}_{[1]} &= \tfrac{(x-c^{(i)})}{2}A + \tfrac{a^{(i)2}}{2}B,\\
H^{(i)}_{[2]} &= \left(\tfrac{-a^{(i)2}}{3} + \tfrac{(x-c^{(i)})^2}{6}\right)A + \tfrac{a^{(i)2}(x-c^{(i)})}{2}B,\\
H^{(i)}_{[3]} &= \left(\tfrac{-13a^{(i)2}(x-c^{(i)})}{48} + \tfrac{(x-c^{(i)})^3}{24}\right)A + \left(\tfrac{-a^{(i)4}}{16} + \tfrac{a^{(i)2}(x-c^{(i)})^2}{4}\right)B,\\
H^{(i)}_{[4]} &= \left(\tfrac{a^{(i)4}}{45} - \tfrac{83a^{(i)2}(x-c^{(i)})^2}{720} + \tfrac{(x-c^{(i)})^4}{120}\right)A + \left(\tfrac{-3a^{(i)4}(x-c^{(i)})}{48} + \tfrac{4a^{(i)2}(x-c^{(i)})^3}{48}\right)B,\\
H^{(i)}_{[5]} &= \left(\tfrac{113a^{(i)4}(x-c^{(i)})}{5760} - \tfrac{97a^{(i)2}(x-c^{(i)})^3}{2880} + \tfrac{(x-c^{(i)})^5}{720}\right)A + \left(\tfrac{a^{(i)6}}{384} - \tfrac{3a^{(i)4}(x-c^{(i)})^2}{96} + \tfrac{2a^{(i)2}(x-c^{(i)})^4}{96}\right)B,\\
H^{(i)}_{[6]} &= \left(\tfrac{-a^{(i)6}}{1575} + \tfrac{593a^{(i)4}(x-c^{(i)})^2}{67200} - \tfrac{253a^{(i)2}(x-c^{(i)})^4}{33600} + \tfrac{(x-c^{(i)})^6}{5040}\right)A\\
&\quad + \left(\tfrac{5a^{(i)6}(x-c^{(i)})}{1920} - \tfrac{20a^{(i)4}(x-c^{(i)})^3}{1920} + \tfrac{8a^{(i)2}(x-c^{(i)})^5}{1920}\right)B,\\
H^{(i)}_{[7]} &= \left(\tfrac{-1873a^{(i)6}(x-c^{(i)})}{3225600} + \tfrac{4327a^{(i)4}(x-c^{(i)})^3}{1612800} - \tfrac{551a^{(i)2}(x-c^{(i)})^5}{403200} + \tfrac{(x-c^{(i)})^7}{403200}\right)A\\
&\quad + \left(\tfrac{-a^{(i)8}}{18432} + \tfrac{15a^{(i)6}(x-c^{(i)})^2}{11520} - \tfrac{30a^{(i)4}(x-c^{(i)})^4}{11520} + \tfrac{8a^{(i)2}(x-c^{(i)})^6}{11520}\right)B,\\
H^{(i)}_{[8]} &= \left(\tfrac{a^{(i)8}}{99225} - \tfrac{54511a^{(i)6}(x-c^{(i)})^2}{203212800} + \tfrac{20939a^{(i)4}(x-c^{(i)})^4}{33868800} - \tfrac{5309a^{(i)2}(x-c^{(i)})^6}{25401600} + \tfrac{(x-c^{(i)})^8}{362880}\right)A\\
&\quad + \left(\tfrac{-35a^{(i)8}(x-c^{(i)})}{645120} + \tfrac{280a^{(i)6}(x-c^{(i)})^3}{645120} - \tfrac{336a^{(i)4}(x-c^{(i)})^5}{645120} + \tfrac{64a^{(i)2}(x-c^{(i)})^7}{645120}\right)B,
\end{aligned}
$$

where $A = \sqrt{(x-c^{(i)})^2 + a^{(i)2}}$ and $B = \ln\left((x-c^{(i)}) + \sqrt{(x-c^{(i)})^2 + a^{(i)2}}\right)$.

ACKNOWLEDGEMENTS

The author is grateful to Professor R.I. Tanner for fruitful discussions and for carefully reading the paper and correcting errors. The author would like to thank the referees for their helpful comments.

REFERENCES

1. Dahlquist G, Bjorck A, Anderson N. *Numerical Methods*; Prentice-Hall: New Jersey, 1974.

2. Press WH, Flannery BP, Teukolsky SA, Vetterling WT. *Numerical Recipes in C: The Art of Scientific Computing*; Cambridge University Press: Cambridge, 1988.

3. Viecelli JA. Exponential difference operator approximation for the sixth order Onsager equation. *Journal of Computational Physics* 1983; **5**0: 162-170.

4. Sallam S, El-Hawary HM. A deficient spline function approximation of second-order differential equations. *Applied Mathematical Modelling* 1984; **8**(6): 408-412.

5. Esmail MN, Fawzy T, Ahmed M, Elmoselhi HO. A deficient spline function approximation to fourth-order differential equations. *Applied Mathematical Modelling* 1994; **1**8(12): 658-664.

6. Gutierrez RH, Laura PAA. Vibrations of non-uniform rings studied by means of the differential quadrature method. *Journal of Sound and Vibration* 1995; **1**85(3): 507-513.

7. Wu TY, Liu GR. Application of the generalized differential quadrature rule to sixth-order differential equations. *Communications in Numerical Methods in Engineering* 2000; **1**6: 777-784.

8. Wu TY, Liu GR. The generalized differential quadrature rule for fourth-order differential equations. *International Journal for Numerical Methods in Engineering* 2001; **5**0: 1907-1929.

9. Wu TY, Liu GR. Application of the generalized differential quadrature rule to eighth-order differential equations. *Communications in Numerical Methods in Engineering* 2001; **1**7: 355-364.

10. Bellman R, Casti J. Differential quadrature and long term integration. *Journal of Mathematical Analysis and Application* 1971; **3**4: 235-238.

11. Wood HG, Morton JB. Onsager's pancake approximation for the fluid dynamics of a gas centrifuge. *Journal of Fluid Mechanics* 1980; **1**01(1): 1-31.

12. Kansa EJ. Multiquadrics-A scattered data approximation scheme with applications to computational fluid-dynamics-II. Solutions to parabolic, hyperbolic and elliptic partial differential equations. *Computers and Mathematics with Applications* 1990; **1**9(8/9); 147-161.

13. Sharan M, Kansa EJ, Gupta S. Application of the multiquadric method for numerical solution of elliptic partial differential equations. *Journal of Applied Science and Computation* 1997; **8**4: 275-302.

14. Zerroukat M, Power H, Chen CS. A numerical method for heat transfer problems using collocation and radial basis functions. *International Journal for Numerical Methods in Engineering* 1998; **4**2: 1263-1278.

15. Mai-Duy N, Tran-Cong T. Numerical solution of differential equations using multiquadric radial basis function networks. *Neural Networks* 2001; **1**4(2): 185-199.

16. Mai-Duy N, Tran-Cong T. Numerical solution of Navier-Stokes equations using multiquadric radial basis function networks. *International Journal for Numerical Methods in Fluids* 2001; **3**7: 65-86.

17. Fedoseyev AI, Friedman MJ, Kansa EJ. Improved multiquadric method for elliptic partial differential equations via PDE collocation on the boundary. *Computers & Mathematics with Applications* 2002; **4**3(3-5): 439-455.

18. Mai-Duy N, Tran-Cong T. Approximation of function and its derivatives using radial basis function network methods. *Applied Mathematical Modelling* 2003; **2**7: 197-220.

19. Jin X, Li G, Aluru NR. On the equivalence between least-squares and kernel approximations in meshless methods. *Computer Modeling in Engineering and Sciences* 2001; **2**(4): 447-462.

20. Atluri SN, Shen S. *The Meshless Local Petrov-Galerkin Method*; Tech Science Press: Encino, 2002.

21. Li S, Liu WK. Meshfree and particle methods and their applications. *Applied Mechanics Reviews* 2002; **5**5(1): 1-34.

22. Liu GR. *Mesh Free Methods - Moving Beyond The Finite Element Method*; CRC Press: Boca Raton, 2003.

23. Liu GR, Gu YT. A local radial point interpolation method (LRPIM) for free vibration analyses of 2-D solids. *Journal of Sound and Vibration* 2001; **2**46(1): 29-46.

24. Wang JG, Liu GR. A point interpolation meshless method based on radial basis functions. *International Journal for Numerical Methods in Engineering* 2002; **54**: 1623-1648.

25. Wang JG, Liu GR. On the optimal shape parameters of radial basis functions used for 2-D meshless methods. *Computer Methods in Applied Mechanics and Engineering* 2002; **191**: 2611-2630.

26. Wang JG, Liu GR, Lin P. Numerical analysis of Biot's consolidation process by radial point interpolation method. *International Journal of Solids and Structures* 2002; **39(6)**: 1557-1573.

27. Gu YT, Liu GR. A boundary radial point interpolation method (BRPIM) for 2-D structural analyses. *Structural Engineering and Mechanics* 2003; **15(5)**: 535-550.

28. Wu YL, Liu GR. A meshfree formulation of local radial point interpolation method (LRPIM) for incompressible flow simulation. *Computational Mechanics* 2003; **30(5-6)**: 355-365.

29. Haykin S. *Neural Networks: A Comprehensive Foundation*; Prentice-Hall: New Jersey, 1999.

30. Abramowitz M, Stegun IA. *Handbook of Mathematical Functions*; Dover Publications: New York, 1972.

31. Madych WR, Nelson SA. Multivariate interpolation and conditionally positive definite functions. *Approximation Theory and its Applications* 1989; **4**: 77-89.

32. Madych WR, Nelson SA. Multivariate interpolation and conditionally positive definite functions, II. *Mathematics of Computation* 1990; **5**4(189): 211-230.

33. Kelkar VS, Sewell RT. *Fundamentals of the Analysis and Design of Shell Structures*; Prentice-Hall, Inc.: New Jersey, 1987.

Table 1: Fourth order ODE, free vibration, pinned-pinned beam: eigenvalues. For each eigenvalue λ_i, the error is consistently reduced with increasing density.

Density	λ_1(error %)	λ_2(error %)	λ_3(error %)	λ_4(error %)	λ_5(error %)
6	3.1415(0.003)	6.2824(0.012)	9.2931(1.397)	11.7987(6.109)	—
8	3.1416(0.000)	6.2830(0.003)	9.4224(0.025)	12.5683(0.015)	15.1874(3.314)
10	3.1416(0.000)	6.2831(0.001)	9.4243(0.005)	12.5657(0.005)	15.7002(0.049)
12	3.1416(0.000)	6.2832(0.000)	9.4246(0.002)	12.5660(0.003)	15.7066(0.008)
Analytic	3.1416	6.2832	9.4248	12.5664	15.7080

Table 2: Fourth order ODE, free vibration, clamped-clamped beam: eigenvalues. For each eigenvalue λ_i, the error is consistently reduced with increasing density.

Density	λ_1(error %)	λ_2(error %)	λ_3(error %)	λ_4(error %)	λ_5(error %)
6	4.7301(0.002)	7.8535(0.003)	10.9136(0.745)	13.0601(7.618)	—
8	4.7300(0.000)	7.8531(0.001)	10.9959(0.002)	14.1633(0.184)	16.8616(2.414)
10	4.7300(0.000)	7.8532(0.000)	10.9955(0.000)	14.1374(0.001)	17.2916(0.074)
12	4.7300(0.000)	7.8532(0.000)	10.9956(0.000)	14.1370(0.001)	17.2791(0.001)
Analytic	4.7300	7.8532	10.9956	14.1372	17.2788

Table 3: Fourth order ODE, free vibration, clamped-pinned beam: eigenvalues. For each eigenvalue λ_i, the error is consistently reduced with increasing density.

Density	λ_1(error %)	λ_2(error %)	λ_3(error %)	λ_4(error %)	λ_5(error %)
6	3.9265(0.002)	7.0669(0.038)	10.0603(1.468)	12.5644(5.897)	—
8	3.9266(0.000)	7.0684(0.016)	10.2088(0.013)	13.3464(0.040)	15.9508(3.289)
10	3.9266(0.000)	7.0685(0.015)	10.2098(0.003)	13.3510(0.005)	16.4941(0.004)
12	3.9266(0.000)	7.0686(0.014)	10.2101(0.000)	13.3514(0.002)	16.4929(0.003)
Analytic	3.9266	7.0696	10.2102	13.3518	16.4934

Table 4: Sixth order ODE, vibration, non-uniform ring with constraints (Figure 7-a): fundamental frequency coefficients.

r	IRBFN(I) and GDQR(G)					Rayleigh-Ritz	DQM
	$n = 7$	8	9	10	11		
1.0	(I) 2.2668	2.2667	2.2667	2.2667	2.2667	2.274	2.268
	(G) 2.2631	2.2669	2.2667	2.2667	2.2667		
1.1	(I) 2.4137	2.4137	2.4137	2.4137	2.4137	2.416	2.417
	(G) 2.4133	2.4137	2.4137	2.4137	2.4137		
1.2	(I) 2.5569	2.5569	2.5568	2.5568	2.5568	2.557	2.561
	(G) 2.5597	2.5565	2.5567	2.5568	2.5568		
1.3	(I) 2.6978	2.6976	2.6968	2.6967	2.6966	2.697	2.701
	(G) 2.7139	2.6944	2.6962	2.6966	2.6966		
1.4	(I) 2.8401	2.8380	2.8344	2.8342	2.8337	2.834	2.839
	(G) 2.8946	2.8242	2.8318	2.8336	2.8335		
1.5	(I) 2.9951	2.9835	2.9711	2.9701	2.9685	2.970	2.976
	(G) 3.1297	2.9407	2.9623	2.9681	2.9678		

Table 5: Sixth order ODE, vibration, non-uniform ring without constraints (Figure 7-b): fundamental frequency coefficients.

r		IRBFN(I) and GDQR(G)					Rayleigh-Ritz	DQM
		$n = 6$	7	8	9	10		
1.0	(I)	2.6831	2.6832	2.6833	2.6833	2.6833	2.687	2.686
	(G)	2.6828	2.6833	2.6833	2.6833	2.6833		
1.1	(I)	2.8452	2.8452	2.8452	2.8452	2.8452	2.846	2.849
	(G)	2.8452	2.8452	2.8452	2.8452	2.8452		
1.2	(I)	3.0060	3.0062	3.0062	3.0062	3.0062	3.006	3.010
	(G)	3.0062	3.0062	3.0062	3.0062	3.0062		
1.3	(I)	3.1656	3.1664	3.1663	3.1664	3.1664	3.167	3.171
	(G)	3.1666	3.1665	3.1665	3.1665	3.1665		
1.4	(I)	3.3241	3.3261	3.3259	3.3262	3.3262	3.326	3.332
	(G)	3.3267	3.3263	3.3262	3.3263	3.3263		
1.5	(I)	3.4827	3.4855	3.4852	3.4857	3.4856	3.486	3.493
	(G)	3.4861	3.4858	3.4857	3.4858	3.4858		

Table 6: Eight order ODE, simply supported single barrel with free edges, 5 training points: final stress resultants.

ϕ (deg)	$M_\phi/\sin\frac{\pi x}{L}$ (lb-ft/ft)		$Q_\phi/\sin\frac{\pi x}{L}$ (lb/ft)		$N_\phi/\sin\frac{\pi x}{L}$ (lb/ft)		$N_{x\phi}/\sin\frac{\pi x}{L}$ (lb/ft)		$N_x/\sin\frac{\pi x}{L}$ (lb/ft)	
	IRBFN	Error(%)	IRBFN	Error(%)	IRBFN	Error(%)	IRBFN	Error(%)	IRBFN	Error(%)
-40	-0.00	0.0000	0.00	0.0000	-0.00	0.0000	-0.00	0.0000	41252.69	0.0672
-20	-488.67	0.0117	-172.86	0.0192	-969.93	0.0077	-4467.04	0.0245	-5839.36	0.0840
0	-958.31	0.0173	-0.00	0.0000	-1739.27	0.0113	-0.00	0.0000	-17376.61	0.0359
20	-488.67	0.0117	172.86	0.0192	-969.93	0.0077	4467.04	0.0245	-5839.36	0.0840
40	0.00	0.0000	0.00	0.0000	0.00	0.0000	0.00	0.0000	41252.69	0.0672

Table 7: Eight order ODE, simply supported single barrel with free edges, 9 training points: final stress resultants.

ϕ (deg)	$M_\phi/\sin\frac{\pi x}{L}$ (lb-ft/ft)		$Q_\phi/\sin\frac{\pi x}{L}$ (lb/ft)		$N_\phi/\sin\frac{\pi x}{L}$ (lb/ft)		$N_{x\phi}/\sin\frac{\pi x}{L}$ (lb/ft)		$N_x/\sin\frac{\pi x}{L}$ (lb/ft)	
	IRBFN	Error(%)	IRBFN	Error(%)	IRBFN	Error(%)	IRBFN	Error(%)	IRBFN	Error(%)
-40	0.00	0.0000	0.00	0.0000	0.00	0.0000	-0.00	0.0000	41225.23	0.0006
-30	-143.96	0.0000	-125.67	0.0000	-302.88	0.0001	-4129.26	0.0001	11690.02	0.0004
-20	-488.72	0.0000	-172.89	0.0000	-969.86	0.0000	-4468.13	0.0000	-5834.45	0.0002
-10	-823.00	0.0000	-118.48	0.0000	-1528.93	0.0000	-2693.36	0.0000	-14717.71	0.0000
0	-958.48	0.0000	-0.00	0.0000	-1739.47	0.0000	-0.00	0.0000	-17382.85	0.0000
10	-823.00	0.0000	118.48	0.0000	-1528.93	0.0000	2693.36	0.0000	-14717.71	0.0000
20	-488.72	0.0000	172.89	0.0000	-969.86	0.0000	4468.13	0.0000	-5834.45	0.0002
30	-143.96	0.0000	125.67	0.0000	-302.88	0.0001	4129.26	0.0001	11690.02	0.0004
40	-0.00	0.0000	-0.00	0.0000	0.00	0.0000	0.00	0.0000	41225.23	0.0006

Table 8: Eight order ODE, simply supported single barrel with free edges, 13 training points: final stress resultants.

ϕ (deg)	$M_\phi/\sin\frac{\pi x}{L}$ (lb-ft/ft)		$Q_\phi/\sin\frac{\pi x}{L}$ (lb/ft)		$N_\phi/\sin\frac{\pi x}{L}$ (lb/ft)		$N_{x\phi}/\sin\frac{\pi x}{L}$ (lb/ft)		$N_x/\sin\frac{\pi x}{L}$ (lb/ft)	
	IRBFN	Error(%)	IRBFN	Error(%)	IRBFN	Error(%)	IRBFN	Error(%)	IRBFN	Error(%)
-40.0	0.00	0.0000	-0.00	0.0000	0.00	0.0000	-0.00	0.0000	41225.02	0.0000
-33.3	-65.48	0.0000	-88.78	0.0000	-129.87	0.0000	-3273.16	0.0000	20019.75	0.0000
-26.7	-245.93	0.0000	-152.98	0.0000	-513.72	0.0000	-4569.10	0.0000	4692.45	0.0000
-20.0	-488.72	0.0000	-172.89	0.0000	-969.86	0.0000	-4468.13	0.0000	-5834.46	0.0000
-13.3	-726.17	0.0000	-146.42	0.0000	-1373.34	0.0000	-3437.96	0.0000	-12540.31	0.0000
-6.7	-896.71	0.0000	-83.21	0.0000	-1644.46	0.0000	-1849.07	0.0000	-16217.26	0.0000
0.0	-958.48	0.0000	-0.00	0.0000	-1739.47	0.0000	-0.00	0.0000	-17382.86	0.0000
6.7	-896.71	0.0000	83.21	0.0000	-1644.46	0.0000	1849.07	0.0000	-16217.26	0.0000
13.3	-726.17	0.0000	146.42	0.0000	-1373.34	0.0000	3437.96	0.0000	-12540.31	0.0000
20.0	-488.72	0.0000	172.89	0.0000	-969.86	0.0000	4468.13	0.0000	-5834.46	0.0000
26.7	-245.93	0.0000	152.98	0.0000	-513.72	0.0000	4569.10	0.0000	4692.45	0.0000
33.3	-65.48	0.0000	88.78	0.0000	-129.87	0.0000	3273.16	0.0000	20019.75	0.0000
40.0	-0.00	0.0000	0.00	0.0000	-0.00	0.0000	0.00	0.0000	41225.02	0.0000

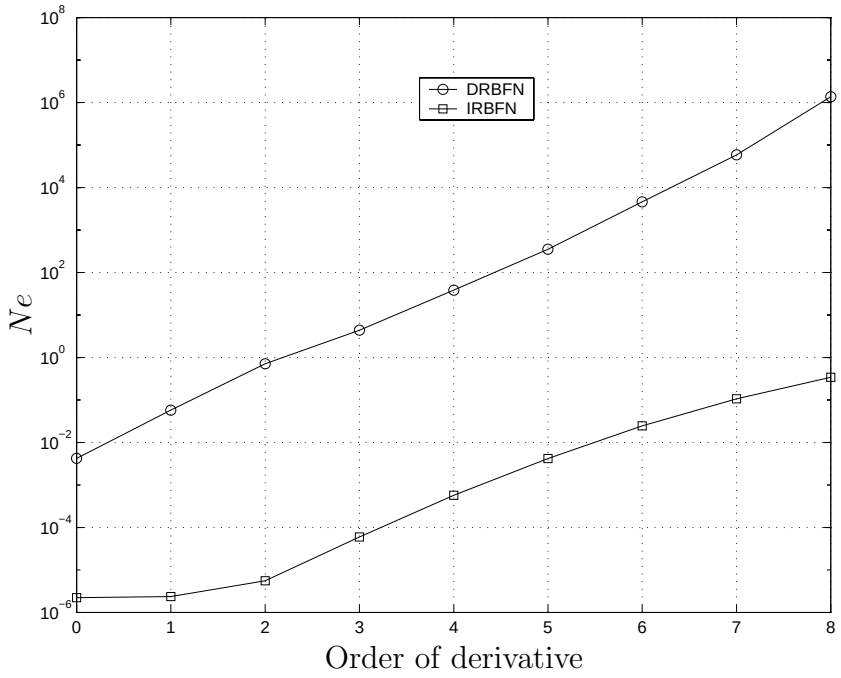

Figure 1: High order derivatives: Comparison of the norm of relative errors of the solution obtained by the IRBFN and the DRBFN. The order of derivatives under consideration here is up to 8 and the value of 0 denotes the target function.

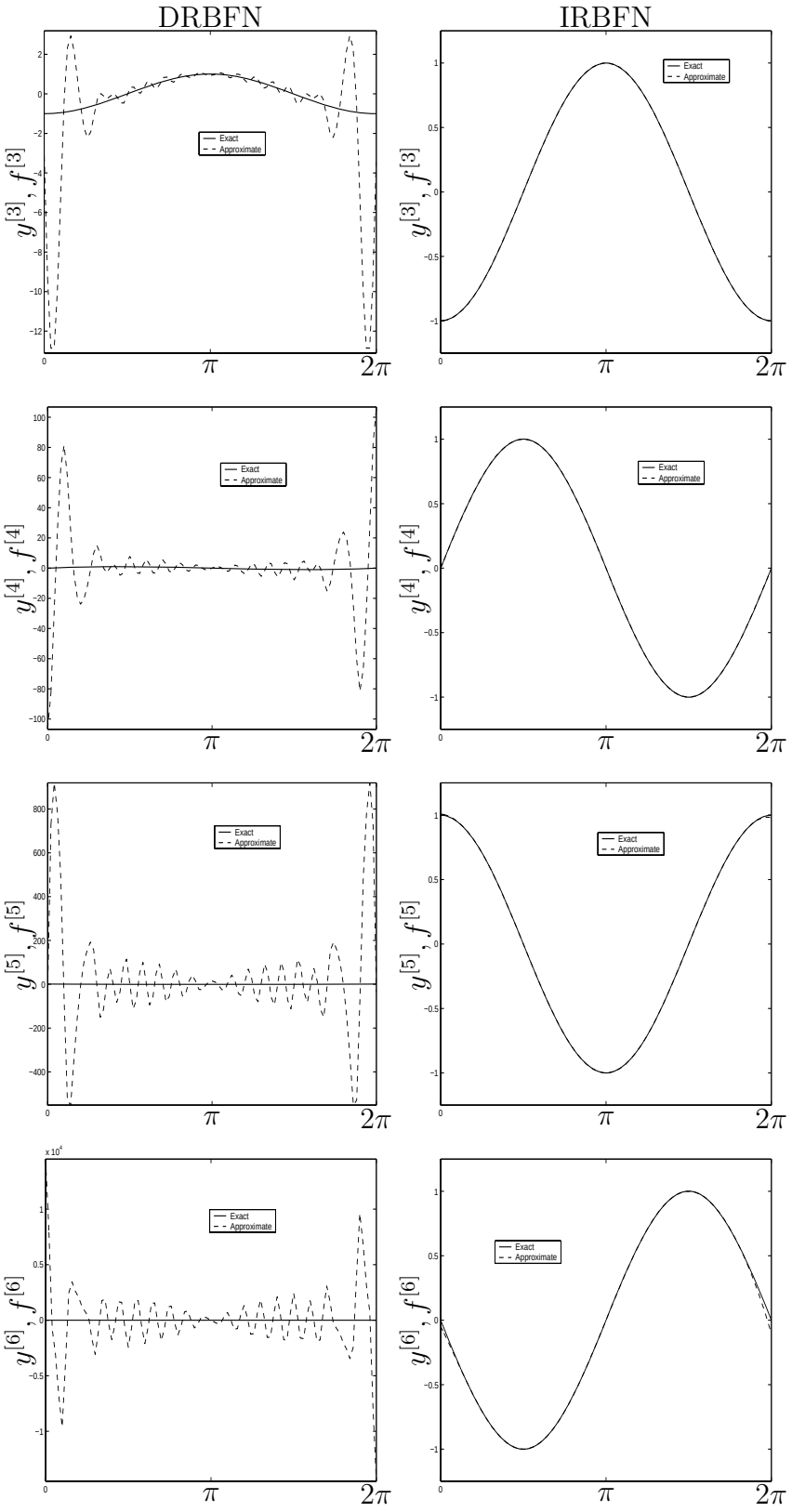

Figure 2: High order derivatives: Plots of some derivatives obtained by the analytical, DRBFN (left) and IRBFN (right) methods. The performance of IRBFN is clearly superior to that of DRBFN.

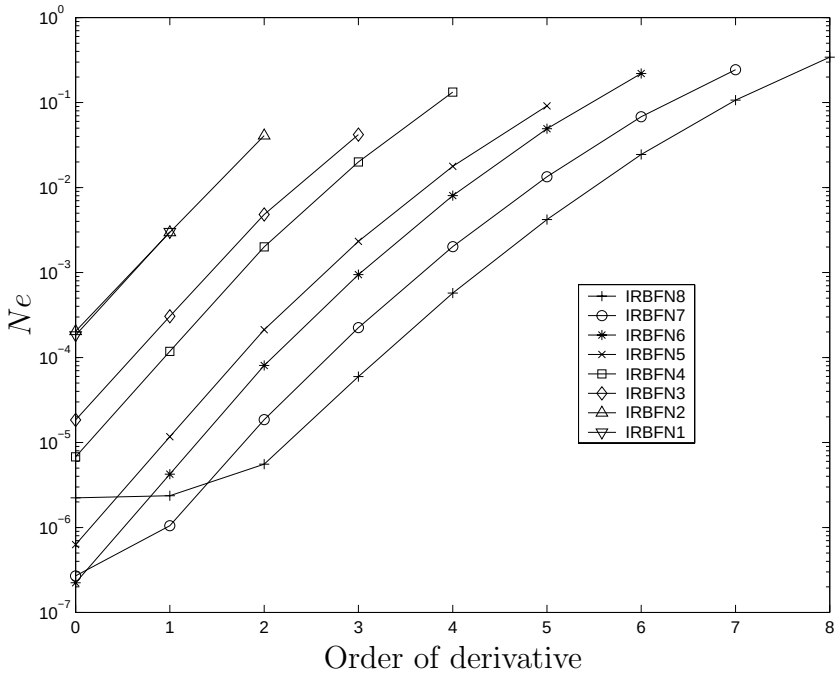

Figure 3: High order derivatives: Effect of the "order" of IRBFN on the solution accuracy. Note that IRBFN-i denotes the indirect scheme starting with the decomposition of ith order derivative into RBFs.

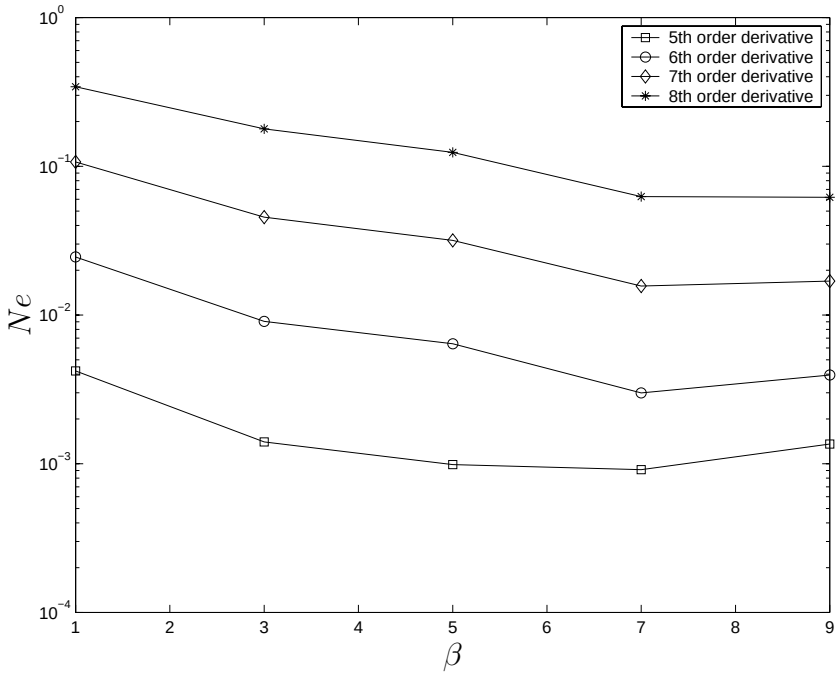

Figure 4: High order derivatives using IRBFN-8 scheme: Effect of β (RBF width) on the accuracy of numerical solution. Better accuracy is obtained with an increase in the value of β up to 7 here.

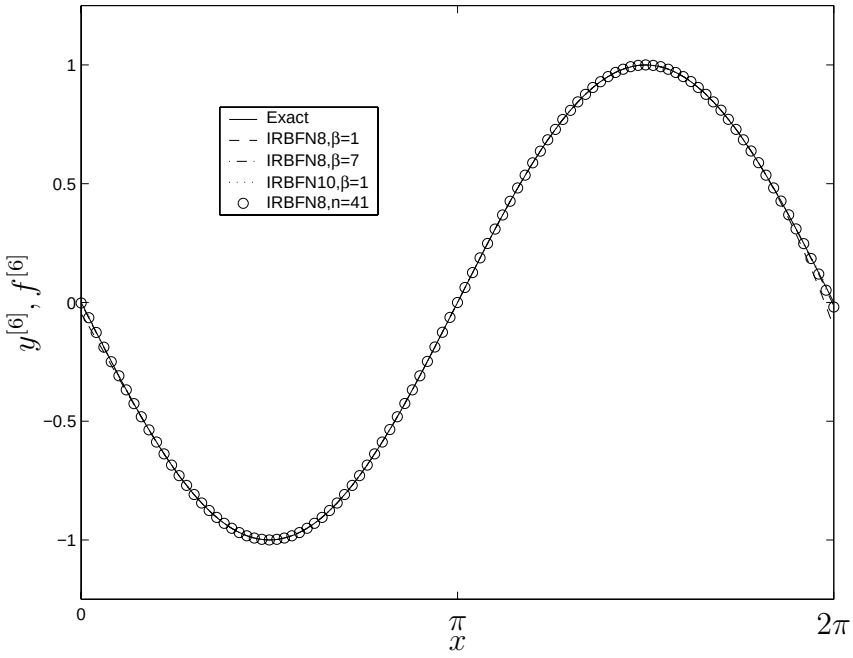

Figure 5: High order derivatives: Approximation of 6th order derivative can be improved by a) increasing the value of β, b) increasing the order of IRBFN or c) increasing a number of centres. New approximate solutions are closer to the exact one. The corresponding error-nomrs are reduced from 0.0245 (IRBFN-8, $\beta = 1$) to 0.0030 (IRBFN-8, $\beta = 7$), 0.0022 (IRBFN-10, $\beta = 1$) and 0.0033 (IRBFN-8, $\beta = 1, n = 41$).

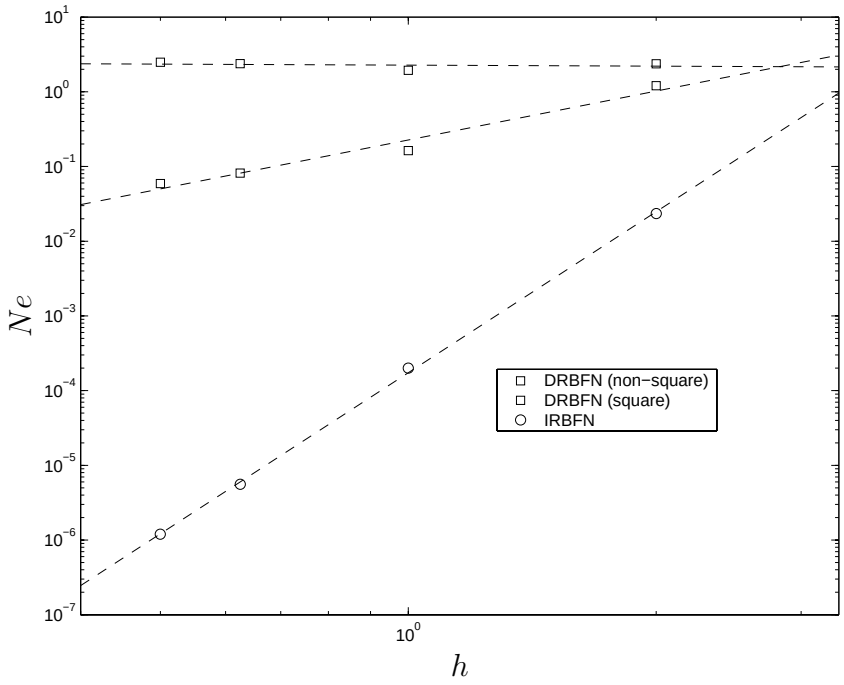

Figure 6: Fourth order ODE, boundary value problem: Comparison of solution accuracy and convergence rate obtained by the unsymmetric DRBF (over-determined and determined system) and IRBF collocation methods, where h is the centre spacing. The latter performs much better than the former in both accuracy and convergence rate.

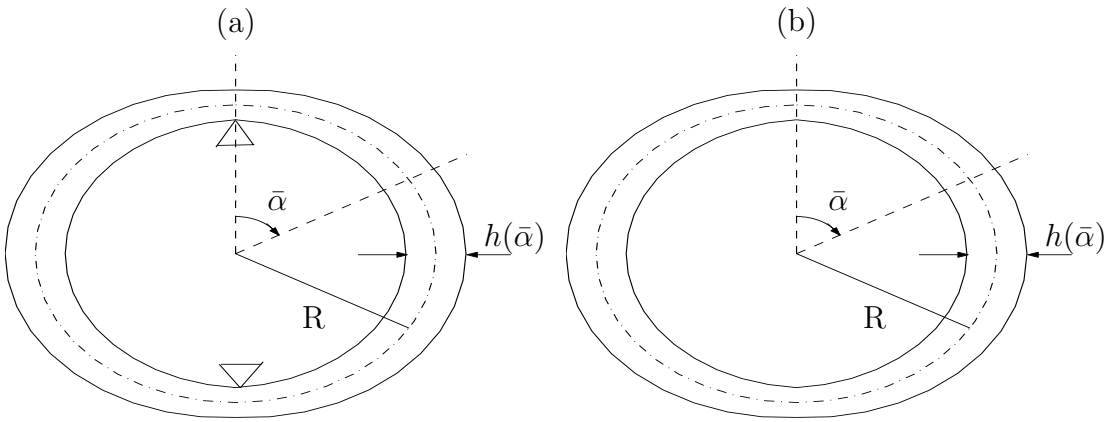

Figure 7: Non-uniform rings

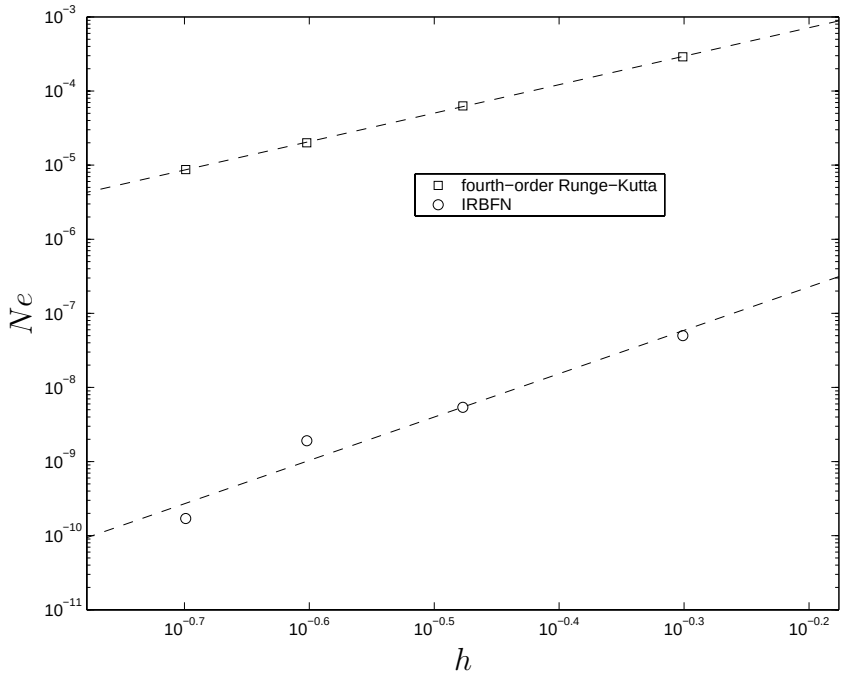

Figure 8: Eighth order ODE, initial value problem: Comparison of the solution accuracy of the IRBF collocation method and that of the traditional fourth-order Runge-Kutta method. The x-axis represents the centre spacing (time step) denoted by h. Both methods yield accurate results and high rate of convergence. The IRBF collocation method achieves error-norms at least three order lower than the Runge-Kutta method.

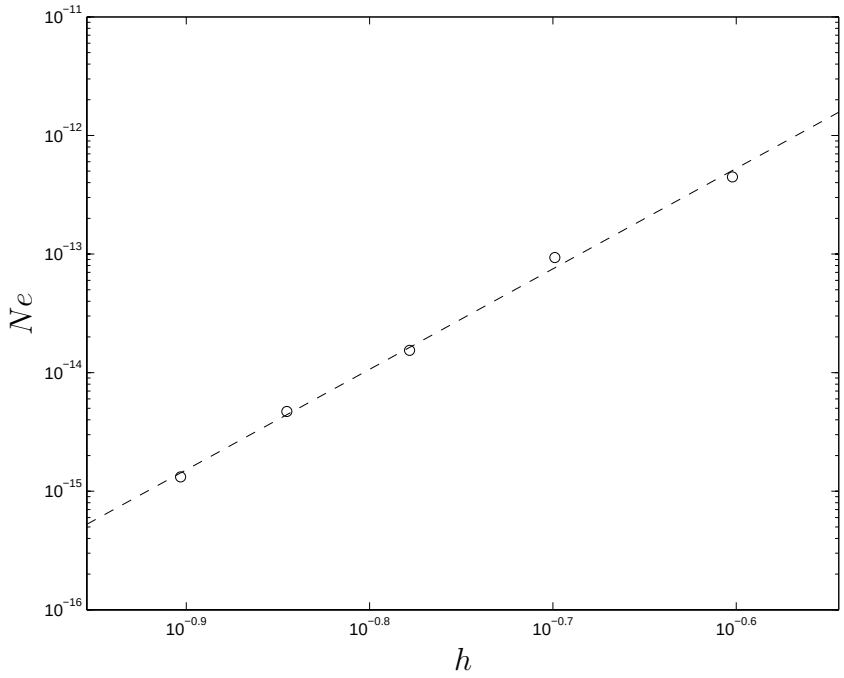

Figure 9: Eighth order ODE, boundary value problem: high convergence rate achieved with the proposed method. The IRBF solution converges apparently as $O(h^{8.4703})$, where h is the centre spacing.

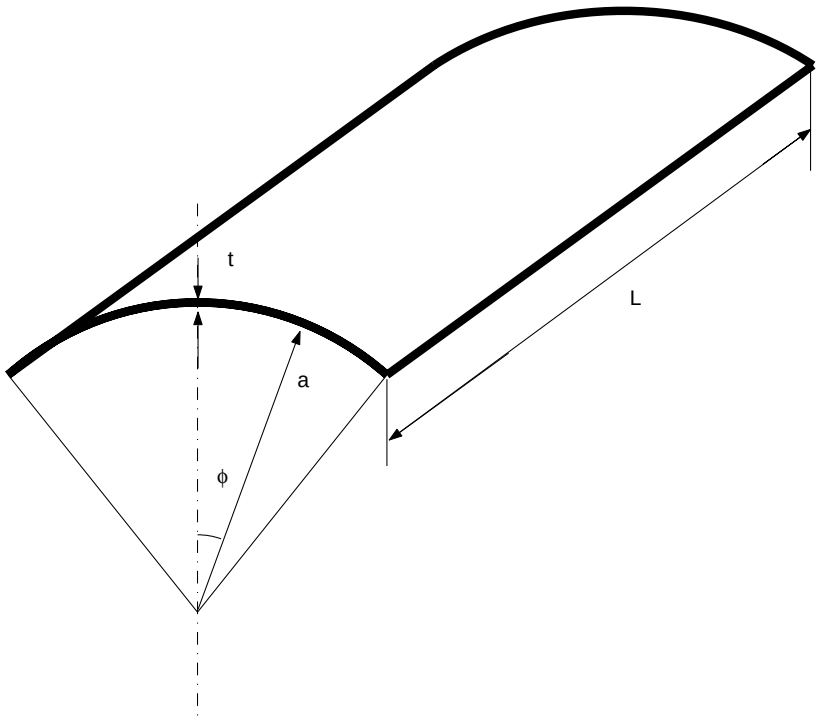

Figure 10: Eighth order ODE: Simply supported single-barrel with free edges.